Instabilities of Isotropic Solutions of Active Polar Filaments

Tanniemola B. Liverpool[1,3] and M. Cristina Marchetti[2,3]
[1]*Applied Mathematics, University of Leeds, Leeds LS2 9JT, United Kingdom*
[2]*Physics Department, Syracuse University, Syracuse, New York 13244*
[3]*Kavli Institute of Theoretical Physics, University of California, Santa Barbara, California 93106*
(Received 12 July 2002; published 3 April 2003)

We study the dynamics of an isotropic solution of polar filaments coupled by molecular motors which generate relative motion of the filaments in two and three dimensions. We investigate the stability of the homogeneous state for constant motor concentration taking into account excluded volume and an estimate of entanglement. At low filament density the system develops a *density* instability, while at high density entanglement drives the instability of *orientational* fluctuations.

DOI: 10.1103/PhysRevLett.90.138102 PACS numbers: 87.16.–b, 05.65.+b, 47.54.+r

Cellular biology provides many realizations of pattern formation in dissipative nonequilibrium systems. An example is the collective behavior of the proteins that compose the cytoskeleton of eukaryotic cells. The cytoskeleton provides both the supporting structure of the cell and the vehicle for internal transport processes [1]. It is a network of long protein filaments, mainly microtubules, actin filaments, and intermediate filaments, coupled by smaller proteins, such as molecular motors and cross-linkers. Motor proteins convert chemical energy derived from the hydrolysis of ATP (adenosine triphosphate) into mechanical work, generating forces and motion of the filaments relative to each other in these *active gels.*

Numerous *in vitro* experiments [2–5] have shown that mixtures of filaments and their associated motor proteins self-organize into macroscopic symmetry-breaking structures, including radial arrays or asters and one-dimensional bundles. The nonequilibrium forces that give rise to these structures include the action of molecular motors and the polymerization/depolymerization process of the filaments. Here we focus on the role of motor proteins and assume that the filaments have fixed length — a situation that can be achieved *in vitro* [4]. A few analytical and numerical studies have investigated the emergence of these complex patterns [4–10]. Continuum models of filament/motor systems in two dimensions have been used to show that spatial patterns are obtained as nonequilibrium solutions of the system dynamics [7,9]. These models have ignored either filament diffusion [9] or the motor action on orientational dynamics [7]. A more microscopic approach was taken by Kruse *et al.* who considered a dynamical model for the development of contractile and motile structures in one dimensional polar filament bundles, while ignoring steric and other interactions between the filaments [8,10].

Many open questions remain concerning the role of the physical properties of the filament/motor gel in controlling the formation of self-organized structures. Experiments have indicated that motor properties, such as their processivity — the fraction of time in a cycle a motor remains attached to the filament — strongly influence pattern formation. This is evident by comparing *in vitro* experiments in microtubules-kinesin to those in actin-myosin mixtures. At high motor concentration, microtubule-kinesin mixtures readily organize in a variety of spatial patterns [4,5]. In contrast, the homogeneous state is much more robust in the weakly coupled actin-myosin II systems, where spatially inhomogeneous structures develop only upon depletion of ATP or at much higher filament concentration [11]. The physical characteristics of the filaments, such as their persistence length, may also contribute to the different behavior of these two gels.

In this Letter we generalize a phenomenological model by Kruse *et al.* [8,10] and obtain a set of continuum equations to describe the dynamics and organization of polar filaments driven by molecular motors in an unconfined geometry in (quasi-)two and three dimensions ($d = 2, 3$) [12]. By modeling the motor-filament interaction microscopically, we can determine the magnitude and, most importantly, the sign of the parameters of the continuum equations, which cannot be obtained by symmetry arguments. We consider an isotropic filament solution, include *excluded volume*, and estimate the effects of *entanglement* on the diffusive dynamics. Our result is a phase diagram (Fig. 2) as a function of the filament density and motor properties that is expected to be relevant to the analysis of recent experiments [5,11].

The filaments are modeled as rigid rods of length l and diameter $b \ll l$. Each filament is identified by the position $\mathbf{r}$ of its center of mass and a unit vector $\hat{\mathbf{n}}$ pointing towards the polar end. Taking into account *filament transport,* the normalized filament probability distribution function, $\Psi(\mathbf{r}, \hat{\mathbf{n}}, t)$, obeys a conservation law [13],

$$\partial_t \Psi + \nabla \cdot \mathbf{J} + \mathcal{R} \cdot \mathbf{J}^r = \mathbf{0}, \tag{1}$$

where $\mathcal{R} = \hat{\mathbf{n}} \times \partial_{\hat{\mathbf{n}}}$ is the rotation operator. The translational and rotational currents $\mathbf{J}$ and $\mathbf{J}^r$ are given by

$$J_i = -D_{ij}\partial_j \Psi - \frac{D_{ij}}{k_B T}\Psi \partial_j V_{\mathrm{ex}} + J_i^{\mathrm{act}}, \tag{2}$$

$$J_i^r = -D_r \mathcal{R}_i \Psi - \frac{D_r}{k_B T} \Psi \mathcal{R}_i V_{\text{ex}} + J_i^{r/\text{act}}, \tag{3}$$

where $i = 1, \ldots, d$, $D_{ij} = D_{\|} \hat{n}_i \hat{n}_j + D_{\perp}(\delta_{ij} - \hat{n}_i \hat{n}_j)$ is the translational diffusion tensor, and D_r is the rotational diffusion constant. The potential V_{ex} incorporates excluded volume effects that play an important role in stabilizing time-dependent solutions. It is given by $k_B T$ times the probability of finding another rod in the interaction area of a given rod,

$$V_{\text{ex}}(\mathbf{r}, \hat{\mathbf{n}}_1) = k_B T \int_{\hat{\mathbf{n}}_2} \int_{\boldsymbol{\xi}}' \Psi(\mathbf{r} + \boldsymbol{\xi}, \hat{\mathbf{n}}_2), \tag{4}$$

where the prime restricts the integral to the interaction volume, corresponding to the region where the two filaments touch at at least one point. The volume of this region is $V_{\text{int}} = v_0 \sqrt{1 - (\hat{\mathbf{n}}_1 \cdot \hat{\mathbf{n}}_2)^2}$, with $v_0 = l^2 b^{d-2}$ and $l^2 \sqrt{1 - (\hat{\mathbf{n}}_1 \cdot \hat{\mathbf{n}}_2)^2} > b^2$. The active currents are given by

$$\mathbf{J}^{\text{act}}(\mathbf{r}, \hat{\mathbf{n}}_1) = \int_{\hat{\mathbf{n}}_2} \int_{\boldsymbol{\xi}}' \mathbf{v}(\boldsymbol{\xi}, \hat{\mathbf{n}}_1, \hat{\mathbf{n}}_2) \Psi(\mathbf{r}, \hat{\mathbf{n}}_1) \Psi(\mathbf{r} + \boldsymbol{\xi}, \hat{\mathbf{n}}_2), \tag{5}$$

$$\mathbf{J}^{r/\text{act}}(\mathbf{r}, \hat{\mathbf{n}}_1) = \int_{\hat{\mathbf{n}}_2} \int_{\boldsymbol{\xi}}' \boldsymbol{\omega}(\boldsymbol{\xi}, \hat{\mathbf{n}}_1, \hat{\mathbf{n}}_2) \Psi(\mathbf{r}, \hat{\mathbf{n}}_1) \Psi(\mathbf{r} + \boldsymbol{\xi}, \hat{\mathbf{n}}_2), \tag{6}$$

where $\mathbf{v} = -\dot{\boldsymbol{\xi}}$ and $\boldsymbol{\omega} = \dot{\hat{\mathbf{n}}}_1 - \dot{\hat{\mathbf{n}}}_2$ are the relative linear and angular velocities of two filaments, with the dot denoting a time derivative. The model naturally contains two competing dynamics. The first is the diffusion of hard rods, which at high density must include excluded volume and entanglement. The second is the local driving force coming from the interaction with the motors. This depends on the polarity of the filaments and breaks the $\hat{\mathbf{n}} \to -\hat{\mathbf{n}}$ symmetry of the hard rod fluid, allowing for states of broken symmetry.

In the absence of external forces and torques the total linear and angular velocity of an interacting pair are conserved. This requires $\mathbf{v}(\boldsymbol{\xi}, \hat{\mathbf{n}}_1, \hat{\mathbf{n}}_2) = -\mathbf{v}(-\boldsymbol{\xi}, \hat{\mathbf{n}}_2, \hat{\mathbf{n}}_1)$ and $\boldsymbol{\omega}(\boldsymbol{\xi}, \hat{\mathbf{n}}_1, \hat{\mathbf{n}}_2) = -\boldsymbol{\omega}(-\boldsymbol{\xi}, \hat{\mathbf{n}}_2, \hat{\mathbf{n}}_1)$. Rotational and translational invariance requires $\mathbf{v}(\boldsymbol{\xi}, \hat{\mathbf{n}}_1, \hat{\mathbf{n}}_2) = -\mathbf{v}(-\boldsymbol{\xi}, -\hat{\mathbf{n}}_1, -\hat{\mathbf{n}}_2)$ and $\boldsymbol{\omega}(\boldsymbol{\xi}, \hat{\mathbf{n}}_1, \hat{\mathbf{n}}_2) = \boldsymbol{\omega}(-\boldsymbol{\xi}, -\hat{\mathbf{n}}_1, -\hat{\mathbf{n}}_2)$. The simplest form for the velocities can be written as

$$\mathbf{v} = \frac{\alpha}{2l} \frac{\boldsymbol{\xi}(1 + \hat{\mathbf{n}}_1 \cdot \hat{\mathbf{n}}_2)}{\sqrt{1 - (\hat{\mathbf{n}}_1 \cdot \hat{\mathbf{n}}_2)^2}} + \frac{\beta}{2} \frac{\hat{\mathbf{n}}_2 - \hat{\mathbf{n}}_1}{\sqrt{1 - (\hat{\mathbf{n}}_1 \cdot \hat{\mathbf{n}}_2)^2}}, \tag{7}$$

$$\boldsymbol{\omega} = \gamma(\hat{\mathbf{n}}_1 \cdot \hat{\mathbf{n}}_2) \frac{\hat{\mathbf{n}}_1 \times \hat{\mathbf{n}}_2}{\sqrt{1 - (\hat{\mathbf{n}}_1 \cdot \hat{\mathbf{n}}_2)^2}}. \tag{8}$$

The velocities have been normalized with the volume of interaction. The parameters α, β, and γ are the rates for the various motor-induced translations and rotations. The contribution proportional to α depends on the separation of the centers of the filaments and results from a difference in motor activity between the ends and midpoints of the filaments. It tends to align the centers of mass and polar heads of the pair [see Fig. 1(a)]. The contribution proportional to β vanishes for aligned filaments and can separate antiparallel filaments, as illustrated in Fig. 1(b). This mechanism yields both translational and rotational currents. The prefactor $(\hat{\mathbf{n}}_1 \cdot \hat{\mathbf{n}}_2)$ in the angular velocity guarantees that motors preferentially bind to two filaments that are at an angle smaller than $\pi/2$. The γ term has no effect on perpendicular filaments. To estimate the rates α, β, and γ, we assume that the motors form small [14] clusters of well defined mean size. The clusters cross-link two filaments, but only one of the motors in a cluster advances on a given filament. The speed of the motor depends on its position along the filament (although our estimate does not depend on the detailed functional form) and vanishes at the polar end, where the motors stall. Assuming a uniform motor "cluster" density, ρ_m, from simple mechanical models of motors [1], we estimate $\alpha \simeq \beta \simeq \gamma l \simeq \rho_m l b^2 \phi(s_c/\tau_c)$, with s_c the motor step length per cycle, τ_c the time for one cycle, and ϕ the duty ratio.

To describe the filament dynamics on length scales large compared to their length, l, we expand the concentration of filaments $\Psi(\mathbf{r} + \boldsymbol{\xi}, \hat{\mathbf{n}}_2)$ near its value at $\mathbf{r}$,

$$\Psi(\mathbf{r} + \boldsymbol{\xi}, \hat{\mathbf{n}}_2) = \Psi(\mathbf{r}, \hat{\mathbf{n}}_2) + \xi_n \hat{\mathbf{e}}_n \cdot \nabla \Psi(\mathbf{r}, \hat{\mathbf{n}}_2) + \tfrac{1}{2} \xi_n \xi_m (\hat{\mathbf{e}}_n \cdot \nabla)(\hat{\mathbf{e}}_m \cdot \nabla) \Psi(\mathbf{r}, \hat{\mathbf{n}}_2) + O(\xi^3). \tag{9}$$

We have introduced a set of orthogonal unit vectors,

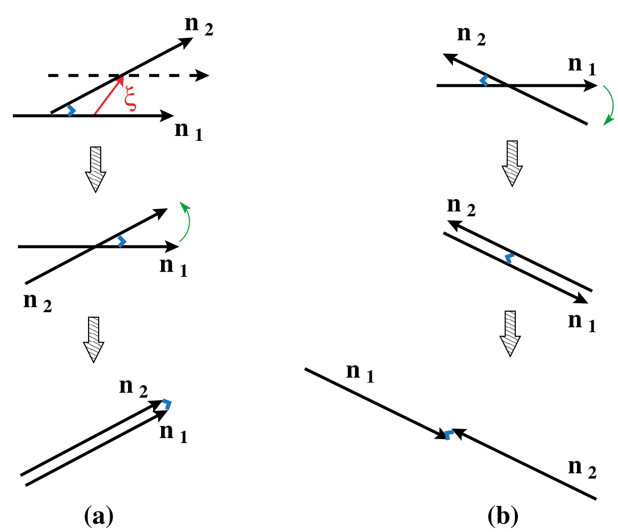

FIG. 1 (color online). Cartoons of motor-induced filament interactions, viewed from the rest frame of filament 2. The angular bracket connecting each pair of filaments represents the motor. (a) An interaction that results in aligned filaments. It can be thought of as a translation at rate α along the direction of the relative filament separation, $\boldsymbol{\xi}$, followed by a counterclockwise rotation of filament 1 about its center of mass at a rate γ. (b) An interaction that results in antialigned filaments. It can be thought of as a clockwise rotation of filament 1 at a rate γ, followed by a translation along the direction of $\hat{\mathbf{n}}_2 - \hat{\mathbf{n}}_1$ at a rate β.

$(\hat{\mathbf{e}}_1, \hat{\mathbf{e}}_2, \hat{\mathbf{z}})$, that provides a natural coordinate system for the problem. The unit vector $\hat{\mathbf{z}}$ is normal to the plane passing through the point of contact of the two filaments and containing the unit vectors $\hat{\mathbf{n}}_1$ and $\hat{\mathbf{n}}_2$. The vectors $\hat{\mathbf{e}}_1 = (\hat{\mathbf{n}}_1 + \hat{\mathbf{n}}_2)/|\hat{\mathbf{n}}_1 + \hat{\mathbf{n}}_2|$ and $\hat{\mathbf{e}}_2 = \mathrm{sgn}(\hat{\mathbf{n}}_1 \cdot \hat{\mathbf{n}}_2)(\hat{\mathbf{n}}_2 - \hat{\mathbf{n}}_1)/|\hat{\mathbf{n}}_2 \cdot \hat{\mathbf{n}}_1|$ are orthogonal unit vectors in this plane. Neglecting the out-of-plane separation (of order b) between the centers of mass of the two filaments, the vector $\boldsymbol{\xi}$ is written in this coordinate system as $\boldsymbol{\xi} = \xi_n \hat{\mathbf{e}}_n$, where summation over $n = 1, 2$ is intended. We assume that on large scales the filament dynamics can be described in terms of the filaments density $\rho(\mathbf{r})$ and the local filament orientation $\mathbf{t}(\mathbf{r})$ defined as the first two moments of the distribution $\Psi(\mathbf{r}, \hat{\mathbf{r}}, t)$,

$$\begin{pmatrix} \rho(\mathbf{r}, t) \\ \mathbf{t}(\mathbf{r}, t) \end{pmatrix} = \int d\hat{\mathbf{n}} \begin{pmatrix} 1 \\ \hat{\mathbf{n}} \end{pmatrix} \Psi(\mathbf{r}, \hat{\mathbf{n}}, t). \tag{10}$$

Coarse-grained equations for ρ and $\mathbf{t}$ can be obtained by inserting Eq. (9) in the expressions for the active currents and for V_{ex}, writing the density $\Psi(\mathbf{r}, \hat{\mathbf{n}}, t)$ in the form of an exact moment expansion, and retaining only the first two moments in this expansion. For brevity, we display here only the dynamical equations linearized about a homogeneous state, with constant density ρ_0 and an isotropic orientational distribution of filaments, corresponding to $\mathbf{t} = 0$. The full and rather cumbersome nonlinear equations will be given elsewhere [15]. Letting $\rho = \rho_0 + \delta\rho$ and keeping only terms up to third order in the gradients, the linearized equations are given by

$$\partial_t \delta\rho = \frac{1}{d}[D_\parallel + (d-1)D_\perp](1 + v_0\rho_0)\nabla^2\delta\rho - \frac{\alpha l v_0 \rho_0}{12d}\nabla^2\delta\rho - \frac{\beta l^2 v_0 \rho_0 (2d+1)}{24d(d+2)}\nabla^2(\boldsymbol{\nabla}\cdot\mathbf{t}), \tag{11}$$

$$\begin{aligned} \partial_t t_i = &- D_r t_i + \frac{1}{d+2}[(d+1)D_\perp + D_\parallel]\nabla^2 t_i + \frac{2}{d+2}(D_\parallel - D_\perp)\partial_i \nabla\cdot\mathbf{t} \\ &- \frac{\alpha l v_0 \rho_0}{12d(d+2)}[\nabla^2 t_i + 2\partial_i \boldsymbol{\nabla}\cdot\mathbf{t}] + \frac{\beta v_0 \rho_0}{d}\partial_i \delta\rho + \frac{\beta l^2 v_0 \rho_0 (2d+1)}{24d^2(d+2)}\partial_i \nabla^2 \delta\rho. \end{aligned} \tag{12}$$

The local orientation is not a conserved variable and decays at a rate $\sim D_r$. Both equations display the competition of diffusive terms ($\propto D\nabla^2$) and pattern-forming terms ($\propto -\alpha\nabla^2$). The linear instability of the homogeneous state occurs when the pattern-forming terms dominate. To linear order, the contribution from the rotational current (proportional to γ) vanishes and excluded volume corrections appear only in the density equation.

To study the linear stability of the homogeneous state, we expand the fields in Fourier components, $\delta\rho(\mathbf{r}) = \sum_{\mathbf{k}} \rho_{\mathbf{k}} e^{i\mathbf{k}\cdot\mathbf{r}}$ and $\mathbf{t}(\mathbf{r}) = \sum_{\mathbf{k}} \mathbf{t}_{\mathbf{k}} e^{i\mathbf{k}\cdot\mathbf{r}}$, and separate $\mathbf{t}_{\mathbf{k}}$ in its component longitudinal and transverse to $\mathbf{k}$, namely $t^L_{\mathbf{k}} = \hat{\mathbf{k}} \cdot \mathbf{t}_{\mathbf{k}}$ and $t^T_{\mathbf{k}} = \hat{\mathbf{k}} \times \mathbf{t}_{\mathbf{k}}$, with $\hat{\mathbf{k}} = \mathbf{k}/|\mathbf{k}|$. In d dimensions there are $d-1$ degenerate transverse modes describing the decay of fluctuations in $t^T_{\mathbf{k}}$, with rate

$$\lambda_T(k) = -D_r - \frac{k^2}{d+2}\left[(d+1)D_\perp + D_\parallel - \frac{\alpha l v_0 \rho_0}{12d}\right]. \tag{13}$$

There are two coupled modes describing the decay of density and $t^L_{\mathbf{k}}$ fluctuations, given by

$$\lambda_\pm(k) = \tfrac{1}{2}\{M_{11} + M_{22} \pm \sqrt{(M_{11} - M_{22})^2 + 4M_{12}M_{21}}\}, \tag{14}$$

with

$$M_{11} = -\frac{k^2}{d}\left[[D_\parallel + (d-1)D_\perp](1 + v_0\rho_0) - \frac{\alpha l v_0 \rho_0}{12}\right], \qquad M_{22} = -D_r - \frac{k^2}{d+2}\left[3D_\parallel + (d-1)D_\perp - \frac{\alpha l v_0 \rho_0}{4d}\right],$$
$$M_{12} = ik^3 \frac{\beta l^2 v_0 \rho_0}{24}\frac{2d+1}{d(d+2)}, \qquad M_{21} = ik\frac{\beta v_0 \rho_0}{d}\left(1 - \frac{l^2 k^2}{24}\frac{2d+1}{d(d+2)}\right). \tag{15}$$

To discuss the stability of the homogeneous state, which is controlled by the real part of the largest eigenvalue, we need to specify the various diffusion constants. For dilute solutions of long thin rods these are $D_\perp = D_\parallel/2 = D/2$ and $D_r = 6D/l^2$, with $D = k_B T \ln(l/b)/(2\pi\eta l)$ and η the solvent viscosity [13]. At higher density, the dynamics is modified by the topological constraint that the filaments cannot pass through each other, resulting in entanglement. This strongly suppresses transverse and rotational diffusion. Entanglement affects both the diffusive and the active currents. For a first estimate of its role on the dynamics of active solutions, we incorporate its effect only on the diffusive currents and do so by replacing the various diffusion constants by the values obtained in the literature for the corresponding entangled *passive* system, $D_\perp \simeq D/\{2[1 + c_\perp \tilde{\rho}_0 (l/b)^{d-2}]^2\}$ and $D_r \simeq 6D/\{l^2[1 + c_r \tilde{\rho}_0 (l/b)^{d-2}]^2\}$ with $c_{r,\perp}$ constants of order unity and $D_\parallel$ essentially unaffected by entanglement [13,16].

It is instructive to first consider the case of $\beta = 0$, where the two longitudinal modes are decoupled. The decay rates of density and $t^L_{\mathbf{k}}$ fluctuations are given by $\lambda_\rho = M_{11}$ and $\lambda_L = M_{22}$, respectively. At low density, λ_ρ

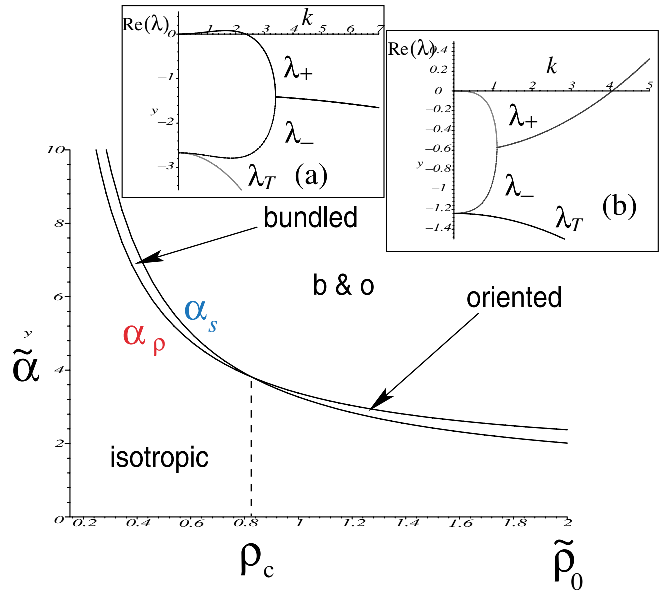

FIG. 2 (color online). Phase diagram for $\beta = 0.4$. For $\tilde{\rho}_0 < \rho_c \approx 0.826$ and $\alpha_\rho < \tilde{\alpha} < \alpha_s$ density fluctuations grow on all scales, while orientational fluctuations are stable ("bundled" state). For $\tilde{\rho}_0 < \rho_c$ and $\alpha_s < \tilde{\alpha} < \alpha_\rho$ short scale orientational fluctuations are unstable, while density fluctuations remains stable ("oriented" state). All modes are unstable for $\tilde{\alpha} > \max(\alpha_\rho, \alpha_s)$. The insets show the modes for (a) $\tilde{\alpha} = 2.95$, $\tilde{\rho}_0 = 1.2$ and (b) $\tilde{\alpha} = 2$, $\tilde{\rho}_0 = 2$.

exceeds λ_L for all k and becomes positive for $\tilde{\alpha} = \alpha l/(8D) > \alpha_\rho(\tilde{\rho}_0)$ on all length scales, with $\alpha_\rho = (3/2) \times \{1 + 1/\tilde{\rho}_0 + 1/[2(1 + \tilde{\rho}_0)]\}$, for $d = 2$ ($c_\perp = c_r = 1$). At high density λ_L exceeds λ_ρ and orientational fluctuations with $k > k_0 \sim (\tilde{\alpha} - \alpha_L)^{-1/2}\tilde{\rho}_0^{-3/2}$ become unstable for $\tilde{\alpha} > \alpha_L(\tilde{\rho}_0) = (3/\tilde{\rho}_0)[1 + (1 + \tilde{\rho}_0)^{-2}/2]$, while density fluctuations can remain stable.

A finite value of $\tilde{\beta} = \beta l/(8D)$ has two effects on the structure of the linear modes. First, the modes can change from diffusive at small k to propagating above a typical wave vector $\sim\tilde{\beta}^{-1/2}$, reflecting the oscillatory behavior arising from the competition between bundling ($\tilde{\alpha}$) and separation ($\tilde{\beta}$). Second, $\tilde{\beta}$ stabilizes the homogeneous state at large length scales. As for $\beta = 0$, at low density the homogeneous state becomes unstable via a *stationary* instability which occurs where the modes are diffusive at $\tilde{\alpha} > \alpha_\rho$ for $k < k_c \sim \tilde{\rho}_0^{-1/2}(1 + \tilde{\rho}_0)^{-1} \times (\alpha - \alpha_\rho)^{1/2}[40\tilde{\beta}^2 + (\alpha_\rho - \tilde{\alpha})(\alpha_L - \tilde{\alpha})]^{-1/2}$. Consideration of the eigenvalue shows that at the largest scales this instability driven by filament bundling ($\tilde{\alpha}$) is associated with density fluctuations. At intermediate scales, where the growth rate is largest, it describes coupled density and orientational fluctuations, suggesting that the "bundled" state may have a definite orientation on short scales. At high density the behavior is controlled by an *oscillatory* instability at $\tilde{\alpha} > \alpha_s = (4\alpha_\rho + 3\alpha_L)/7$ and $k > k'_c \sim \tilde{\rho}_0^{-1/2}(1 + \tilde{\rho}_0)^{-1}(\tilde{\alpha} - \alpha_s)^{-1/2}$, describing the growth of orientational fluctuation. Notice that this instability should eventually be cut off at the smallest length scales (where our continuum theory breaks down) by excluded volume interactions. The phase diagram in the $(\tilde{\alpha}, \tilde{\rho}_0)$ plane is shown in Fig. 2.

The critical values α_ρ and α_s diverge at low density and decrease as $\tilde{\rho}_0$ increases, indicating that entanglement destabilizes the homogeneous state.

More work is needed to understand the nature of the spatially inhomogeneous state. It will also be relatively straightforward to include motor transport which is important for very processive motors and at low motor densities. An inhomogeneous motor density may also be required for the formation of stable asters and vortices at low filament concentration. Finally, it will be interesting to study the response of the motor/filament gel to shear.

We thank E. Frey, J. Käs, K. Kruse, F. MacKintosh, A. C. Maggs, D. Morse, and S. Ramaswamy for many helpful discussions. This research was supported in part by the National Science Foundation under Grants No. PHY99-07949 (at KITP) and No. DMR97-30678 (at Syracuse) and the Royal Society (London).

[1] J. Howard, *Mechanics of Motor Proteins and the Cytoskeleton* (Sinauer, New York, 2000).
[2] K. Takiguchi, J. Biochem. (Tokyo) **109**, 520 (1991); R. Urrutia *et al.*, Proc. Natl. Acad. Sci. U.S.A. **88**, 6701 (1991).
[3] D. Humphrey, C. Duggan, D. Saha, D. Smith, and J. Käs, Nature (London) **416**, 413 (2002).
[4] F. J. Nédélec, T. Surrey, A. C. Maggs, and S. Leibler, Nature (London) **389**, 305 (1997).
[5] T. Surrey, F. J. Nédélec, S. Leibler, and E. Karsenti, Science **292**, 1167 (2001).
[6] H. Nakazawa and K. Sekimoto, J. Phys. Soc. Jpn. **65**, 2404 (1996); K. Sekimoto and H. Nakazawa, in *Current Topics in Physics*, edited by Y. M. Cho, J. B. Homg, and C. N. Yang (World Scientific, Singapore, 1998).
[7] B. Bassetti, M. C. Lagomarsino, and P. Jona, Eur. Phys. J. B **15**, 483 (2000).
[8] K. Kruse and F. Jülicher, Phys. Rev. Lett. **85**, 1779 (2000); cond-mat/0207212.
[9] H. Y. Lee and M. Kardar, Phys. Rev. E **64**, 56113 (2001).
[10] K. Kruse, S. Camalet, and F. Jülicher, Phys. Rev. Lett. **87**, 138101 (2001).
[11] D. Humphrey, C. Duggan, D. Saha, D. Smith, and J. Käs Nature (London) **416**, 413 (2002).
[12] We assume that even in 3D motors induce only relative displacement and rotation within the plane that contains the two cross-linked filaments.
[13] M. Doi and S. F. Edwards, *The Theory of Polymer Dynamics* (Oxford University Press, New York, 1986).
[14] We neglect motor cooperativity within a cluster, which may be important for myosin in muscle fibers.
[15] The full nonlinear equations can be found at http://physics.syr.edu/~mcm/nonlinear_eqs.pdf
[16] I. Teraoka and R. Hayakawa, J. Chem. Phys. **89**, 6989 (1988); **91**, 2643 (1989).